

# Differential Dynamic Programming with Nonlinear Safety Constraints Under System Uncertainties

Gokhan Alcan and Ville Kyrki

**Abstract**—Safe operation of systems such as robots requires them to plan and execute trajectories subject to safety constraints. When those systems are subject to uncertainties in their dynamics, it is challenging to ensure that the constraints are not violated. In this paper, we propose Safe-CDDP, a safe trajectory optimization and control approach for systems under additive uncertainties and non-linear safety constraints based on constrained differential dynamic programming (DDP). The safety of the robot during its motion is formulated as chance constraints with user-chosen probabilities of constraint satisfaction. The chance constraints are transformed into deterministic ones in DDP formulation by constraint tightening. To avoid over-conservatism during constraint tightening, linear control gains of the feedback policy derived from the constrained DDP are used in the approximation of closed-loop uncertainty propagation in prediction. The proposed algorithm is empirically evaluated on three different robot dynamics with up to 12 degrees of freedom in simulation. The computational feasibility and applicability of the approach are demonstrated with a physical hardware implementation.

## I. INTRODUCTION

In many real-world applications, robots are situated in uncertain environments with stochastic dynamics, where they are required to satisfy particular safety constraints such as collision avoidance or physical limits of their actuators. Within this context, *safety* can be defined as the feasibility and stability of a control policy that achieves the requirements of the desired task while satisfying the safety constraints considering uncertainties affecting the system.

Safety in robotics is an active research area and can be studied as trajectory optimization and control under constraints in a stochastic environment. In this context, model predictive control (MPC) is a useful framework, as it allows the optimization of state and input trajectories based on an objective function under chance constraints [1]. In direct optimization of such a problem, chance constraints are typically transformed to deterministic ones by constraint tightening with precomputed fixed controller gains [2] or robust constraints are defined using large confidence bounds of uncertainties [3]. In both cases, the true effect of feedback on uncertainty propagation is generally omitted, which leads to excessive conservatism and related loss of performance.

To address the question of how to avoid the loss of performance related to conservative constraint tightening, we propose a novel safe trajectory optimization and control approach, which we call Safe Constrained Differential

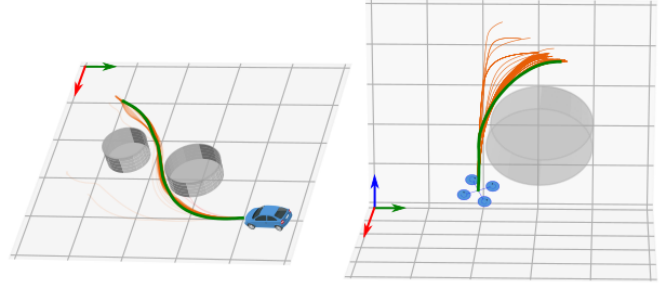


Fig. 1. Safe-CDDP successfully generates optimal trajectories under system uncertainties for complex and underactuated robots. Iteratively generated safe trajectories (orange) and the real trajectories (green) traveled by 2D car-like robot (Left) and 3D quadrotor robot (Right) in constrained environments.

Dynamic Programming (Safe-CDDP). The proposed method extends standard differential dynamic programming (DDP) to handling nonlinear state and input constraints in the presence of additive system uncertainties. The constraints are handled by modeling the problem as a chance-constrained optimal control problem under uncertainty and using constraint tightening [4] to turn it into a deterministic constrained problem, thus generating an appropriate safety margin for the constraints. To reduce the uncertainty in the prediction horizon, we incorporate the control gains of a locally optimal affine feedback policy derived in the backward pass of DDP, which yields a good approximation for optimized trajectories at convergence and avoids excessive conservatism.

To apply the method in real-time feedback control, we also need to address the issue that the tightened constraints are only virtual in the sense that the system noise may cause them to be violated within the safety margin even when they are tightened appropriately. Thus, the utilization of such a constrained formulation in an optimizer creates the risk of a constraint violation, which the optimization process needs to handle appropriately.

The main contributions of our work are:

- 1) A principled way of reflecting the effect of feedback on uncertainty propagation in prediction through the locally optimal control derived in constrained DDP formulation to avoid excessive conservatism.
- 2) A safe model predictive control approach (Safe-CDDP) with general nonlinear constraints in the presence of additive system uncertainties.
- 3) Simulation studies for three types of robot platform dynamics demonstrating that Safe-CDDP ensures stochastic constraint satisfaction for complex and under-actuated robots in safety-required tasks (Fig. 1).
- 4) Validation via hardware implementation for a differen-

This work was financially supported by Academy of Finland (B-REAL project with grant number 328399).

All authors are with Intelligent Robotics Group, Department of Electrical Engineering and Automation (EEA), Aalto University, Espoo, Finland. {gokhan.alcan, ville.kyrki}@aalto.fi

tial drive robot that the proposed method is computationally feasible using a low-power CPU.

Compared to existing formulations to similar problems, the proposed approach simultaneously modes the closed-loop effects of additive uncertainties and includes general nonlinear state constraints.

## II. RELATED WORK

Robust model predictive control approaches involve direct optimization that enables to employ of nonlinear state and input constraints by considering the uncertainty with a worst-case safety bound. Since robust MPC is computationally complex, tube MPCs [5] are designed as an approximation for robust MPCs but they require to define tube geometry dynamics and in some cases time-consuming offline computation [6]. On the other hand, Differential Dynamic Programming (DDP) formulation allows the decomposition of a trajectory optimization problem into smaller ones by limiting the state space to a quadratic trust-region around a current reference solution [7], which results in only local optimality but reduces the processing cost dramatically. Although there is no straightforward way to incorporate nonlinear state and input constraints in the DDP formulation, recent attempts are promising. Next, we provide an overview of previous work related to constrained deterministic and stochastic variants of DDPs.

### A. Constrained Deterministic DDPs

Some recent studies target the design of DDP with input constraints [8], [9], [10]. However, for this work methods that incorporate also state constraints are more relevant. Xie *et al.* [11] utilized Karush-Kuhn-Tucker (KKT) conditions and modified the DDP formulation in the presence of nonlinear state and input constraints according to the active set of constraints at each time step to keep the trajectories feasible. Aoyama *et al.* [12] utilized the work developed in [11] and extended it through an Augmented Lagrangian method by considering a set of penalty functions. Pavlov *et al.* [13] introduced primal-dual interior-point DDP to handle nonlinear state and input constraints. The method is quite promising since it does not require to identify the active set of constraints, but it needs second-order derivatives of the state constraint. Augmented Lagrangian TRajjectory Optimizer (ALTRO) [14] was also recently developed to fuse the advantageous sides of direct methods and DDPs. It handles general deterministic nonlinear state and input constraints with fast convergence and also enables to start with infeasible initial trajectories.

The aforementioned methods achieve promising performances in handling nonlinear constraints and increase the usability of DDPs in robotics tasks. However, in the presence of system uncertainty, they lack safety provisions, which are the primary issue studied in this work.

### B. Stochastic DDPs

Todorov and Li [15] developed input constrained iterative Linear Quadratic Gaussian control for nonlinear stochastic

systems involving multiplicative noise with standard deviation proportional to the control signals. Theodorou *et al.* [16] then extended it to stochastic DDPs for state and control multiplicative process noise. In their work, the derived control policy does not depend on the statistical characteristics of the noise when the stochastic dynamics have only additive noise. Pan and Theodorou [17] introduced a data-driven probabilistic unconstrained DDP using Gaussian processes to address the uncertainty for dynamics models. Celik *et al.* [18] proposed to model state and action physical limits as probabilistic chance constraints in a DDP structure to avoid catastrophic greedy updates. The method does not apply to tasks that need to employ nonlinear constraints on states such as obstacle avoidance, since it involves only linear box-constraints on states and actions as their limits. Ozaki *et al.* [19] proposed a modification for stochastic DDP developed in [16] considering the disturbances and the uncertainties as random state perturbations for an unconstrained deterministic dynamical system and employing unscented transform. They then further improved the method by tube stochastic DDP [20] to handle the control constraints but nonlinear constraints on states were not included.

Our approach widens the extent of stochastic DDPs by considering general nonlinear state and input constraints in the presence of additive uncertainties.

## III. PROPOSED METHOD

We consider a nonlinear discrete-time dynamical system of the form

$$\mathbf{x}_{k+1} = f(\mathbf{x}_k, \mathbf{u}_k) + \omega_k, \quad (1)$$

where  $\mathbf{x}_k \in \mathbb{R}^n$  and  $\mathbf{u}_k \in \mathbb{R}^m$  are the system state and the control input at time step  $k$ , respectively.  $f : \mathbb{R}^n \times \mathbb{R}^m \rightarrow \mathbb{R}^n$  is a nonlinear state transition function which is assumed to be twice differentiable.  $\omega_k$  is assumed to be spatially uncorrelated independent and identically distributed noise, drawn from a zero mean Gaussian distribution with a known covariance matrix,  $\omega_k \sim \mathcal{N}(\mathbf{0}, \Sigma^\omega)$ .

For a given initial state  $\mathbf{x}_0$ , a goal state  $\mathbf{x}_{goal}$ , and a time horizon  $N$ , the aim is to find an input trajectory  $\{\mathbf{u}_0, \dots, \mathbf{u}_{N-1}\}$  that minimizes the expectation of an objective function

$$J(\mathbf{u}_0, \dots, \mathbf{u}_{N-1}) = \ell^f(\mathbf{x}_N) + \sum_{k=0}^{N-1} \ell(\mathbf{x}_k, \mathbf{u}_k), \quad (2)$$

where  $\ell^f : \mathbb{R}^n \rightarrow \mathbb{R}$  and  $\ell : \mathbb{R}^n \times \mathbb{R}^m \rightarrow \mathbb{R}$  are the final cost and the running cost, respectively. By considering the input limitations and external constraints on the states, chance-constrained MPC for this problem can be formulated as

$$\begin{aligned} \min_{\mathbf{u}_0, \dots, \mathbf{u}_{N-1}} \quad & \mathbb{E} \left( J(\mathbf{u}_0, \dots, \mathbf{u}_{N-1}) \right) \\ \text{subject to} \quad & \mathbf{x}_{k+1} = f(\mathbf{x}_k, \mathbf{u}_k) + \omega_k, \\ & \mathbf{u}_{min} \leq \mathbf{u}_k \leq \mathbf{u}_{max}, \\ & \Pr[g(\mathbf{x}_k, \mathbf{u}_k) \leq \mathbf{0}] > \beta_k, \\ & \mathbf{x}_0 = \bar{\mathbf{x}}, \end{aligned} \quad (3)$$

for all  $k = 0, \dots, N - 1$ . Here we simply add box-constraint on control inputs defined by the boundaries  $\mathbf{u}_{min}$  and  $\mathbf{u}_{max}$ .  $\mathbf{g}$  is a vector of  $c$  constraints in the form of differentiable functions representing the deterministic state constraints and  $\beta_k = [\beta_{1,k}, \dots, \beta_{c,k}]$  is a vector of minimum satisfaction probabilities for these constraints for time step  $k$ .

Future predicted states in MPC formulation will result in stochastic distribution due to the noise  $\omega_k$  in state transition. This leads to chance constraints on states, therefore the safety of the predicted trajectory is determined by the probability of constraint satisfaction. Typically, sufficiently safe control actions are desired to cope with the effect of the uncertainties. To achieve this, chance constraints can be converted into deterministic ones by tightening the constraints [21]. Overly conservative tightening based on the propagated uncertainty such as employing open-loop uncertainty propagation narrows dramatically the admissible ranges of the states and can make the optimization intractable or even unsolvable [22] (Fig. 2).

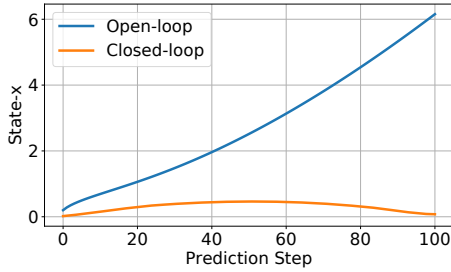


Fig. 2. Open-loop and closed-loop uncertainty ( $2\sigma$ ) propagation through prediction horizon for a simple double integrator system in a constrained trajectory optimization problem.

In order to reflect the effect of feedback on uncertainty propagation in prediction and avoid over-conservatism, we propose the following constrained differential dynamic programming-based model predictive control structure. An initial trajectory is optimized in successive backward and forward passes, while the deterministic constraints are updated periodically in constraint tightening. In each backward pass, the derivatives of the action-value function ( $Q_k(x_k, u_k)$ ) and optimum value function ( $V_k(x_k)$ ) are calculated backward starting from the final step in the horizon ( $N$ ) using the current estimated (or initialized) trajectories and predefined objective function as in (2). In forward passes, the nominal state-control trajectory is updated in forward starting from the initial state by using the derivatives obtained in the backward pass and performing local optimizations considering the constraints. In constraint tightening, chance constraints in (3) are converted into deterministic ones by tightening the constraints using the derived locally optimal control from the backward pass in the uncertainty propagation through prediction. These steps will be detailed in the next sections together with the entire algorithm.

#### A. Backward Pass

The backward pass that follows the formulation in [11] with the assumption of deterministic constraints briefly ex-

plained here for completeness. Using standard DDP formulation, action-value function  $Q_k(\mathbf{x}_k, \mathbf{u}_k)$  can be approximated as a quadratic function as

$$Q(\mathbf{x} + \delta\mathbf{x}, \mathbf{u} + \delta\mathbf{u}) \approx Q + Q_{\mathbf{x}}^{\top} \delta\mathbf{x} + Q_{\mathbf{u}}^{\top} \delta\mathbf{u} + \frac{1}{2}(\delta\mathbf{x}^{\top} Q_{\mathbf{xx}} \delta\mathbf{x} + \delta\mathbf{u}^{\top} Q_{\mathbf{uu}} \delta\mathbf{u}) + \delta\mathbf{x}^{\top} Q_{\mathbf{xu}} \delta\mathbf{u} \quad (4)$$

where  $\delta\mathbf{x}$  and  $\delta\mathbf{u}$  are the deviations about the nominal action-state pair  $(\mathbf{x}, \mathbf{u})$ . The derivatives of  $Q$  function are then

$$\begin{aligned} Q_{\mathbf{x}} &= \ell_{\mathbf{x}} + f_{\mathbf{x}}^{\top} V'_{\mathbf{x}}, \\ Q_{\mathbf{u}} &= \ell_{\mathbf{u}} + f_{\mathbf{u}}^{\top} V'_{\mathbf{x}}, \\ Q_{\mathbf{xx}} &= \ell_{\mathbf{xx}} + f_{\mathbf{x}}^{\top} V'_{\mathbf{xx}} f_{\mathbf{x}} + V'_{\mathbf{x}} f_{\mathbf{xx}}, \\ Q_{\mathbf{uu}} &= \ell_{\mathbf{uu}} + f_{\mathbf{u}}^{\top} V'_{\mathbf{xx}} f_{\mathbf{u}} + V'_{\mathbf{x}} f_{\mathbf{uu}}, \\ Q_{\mathbf{xu}} &= \ell_{\mathbf{xu}} + f_{\mathbf{x}}^{\top} V'_{\mathbf{xx}} f_{\mathbf{u}} + V'_{\mathbf{x}} f_{\mathbf{xu}}. \end{aligned} \quad (5)$$

where  $V$  is the value function (see Appendix for details). Note that to simplify the notations, we dropped the time step indices, used prime to indicate the next time step and used subscripts for the derivatives.

In unconstrained situations, locally optimal control deviations can be computed by minimizing (4) with respect to  $\delta\mathbf{u}$  resulting in

$$\delta\mathbf{u}^* = -Q_{\mathbf{uu}}^{-1}(Q_{\mathbf{ux}}\delta\mathbf{x} + Q_{\mathbf{u}}) \triangleq \bar{\mathbf{K}}\delta\mathbf{x} + \bar{\mathbf{d}} \quad (6)$$

where  $\bar{\mathbf{K}}$  is the linear feedback gain and  $\bar{\mathbf{d}}$  is the affine term.

Under state and/or input constraints, the optimal control problem turns into

$$\begin{aligned} \min_{\delta\mathbf{u}} \quad & Q(\mathbf{x} + \delta\mathbf{x}, \mathbf{u} + \delta\mathbf{u}), \\ \text{subject to} \quad & \mathbf{g}(\mathbf{x} + \delta\mathbf{x}, \mathbf{u} + \delta\mathbf{u}) \leq 0. \end{aligned} \quad (7)$$

where the constraint vector  $\mathbf{g}$  includes the deterministic state constraints obtained in the constraint tightening step (Section III-C) including input limitations. In order to incorporate the constraints in the estimation of action-value function (4), constraints' first order approximations are obtained as

$$\begin{aligned} \mathbf{g}(\mathbf{x} + \delta\mathbf{x}, \mathbf{u} + \delta\mathbf{u}) &\approx \mathbf{g}(\mathbf{x}, \mathbf{u}) \\ &+ \underbrace{\mathbf{g}_{\mathbf{u}}(\mathbf{x}, \mathbf{u}) \delta\mathbf{u}}_{\triangleq \mathbf{C}} + \underbrace{\mathbf{g}_{\mathbf{x}}(\mathbf{x}, \mathbf{u}) \delta\mathbf{x}}_{\triangleq \mathbf{D}} \end{aligned} \quad (8)$$

Xie *et al.* [11] proposed to check the set of active constraints during the iterations to make sure that the analytical approximation of the value function around the nominal trajectories still yields a good approximation. To achieve this, all active constraints *i.e.*, inequality constraints whose boundaries are on the current nominal trajectory and all equality constraints are included in a set and the optimization problem in (7) is converted to

$$\min_{\delta\mathbf{u}} \quad Q_{\mathbf{u}}^{\top} \delta\mathbf{u} + \frac{1}{2}(\delta\mathbf{u}^{\top} Q_{\mathbf{uu}} \delta\mathbf{u}) + \delta\mathbf{x}^{\top} Q_{\mathbf{xu}} \delta\mathbf{u}, \quad (9)$$

subject to  $\mathbf{C}\delta\mathbf{u} = \mathbf{D}\delta\mathbf{x}$ .

An analytical solution to this problem through KKT conditions [23] can be found by solving the pair of equations

$$\begin{aligned} Q_{\mathbf{uu}}\delta\mathbf{u} + Q_{\mathbf{ux}}\delta\mathbf{x} + Q_{\mathbf{u}} + \mathbf{C}^{\top}\boldsymbol{\lambda} &= \mathbf{0} \\ \mathbf{C}\delta\mathbf{u} - \mathbf{D}\delta\mathbf{x} &= \mathbf{0} \end{aligned} \quad (10)$$

where  $\lambda$  is a vector of Lagrangian multipliers. By solving (10) with pruned matrices  $\tilde{\mathbf{C}}$  and  $\tilde{\mathbf{D}}$  that ensures nonexistence of negative  $\lambda$  values (check [11] for details), locally optimal input deviations can be again expressed as a function of state deviations as follows:

$$\delta \mathbf{u}^* = \mathbf{K} \delta \mathbf{x} + \mathbf{d} \quad (11)$$

where the control parameters  $\mathbf{K}$  and  $\mathbf{d}$  are now calculated as

$$\begin{aligned} \mathbf{K} = & -Q_{uu}^{-1}Q_{ux} \\ & -Q_{uu}^{-1}\tilde{\mathbf{C}}^\top(\tilde{\mathbf{C}}Q_{uu}^{-1}\tilde{\mathbf{C}}^\top)^{-1}\tilde{\mathbf{D}} \\ & +Q_{uu}^{-1}\tilde{\mathbf{C}}^\top(\tilde{\mathbf{C}}Q_{uu}^{-1}\tilde{\mathbf{C}}^\top)^{-1}\tilde{\mathbf{C}}Q_{uu}^{-1}Q_{ux}, \\ \mathbf{d} = & -Q_{uu}^{-1}(Q_u - \tilde{\mathbf{C}}^\top(\tilde{\mathbf{C}}Q_{uu}^{-1}\tilde{\mathbf{C}}^\top)^{-1}\tilde{\mathbf{C}}Q_{uu}^{-1}Q_u). \end{aligned} \quad (12)$$

It is observed that  $\delta \mathbf{u}^*$  at time step  $k$  requires the knowledge of first and second derivatives of the value function for next time step  $(k+1)$  as shown in (5). By plugging the optimal control found in (11) into the approximated action-value function (4), the value function can be approximated as

$$V \approx \frac{1}{2}\delta \mathbf{x}^\top V_{xx}\delta \mathbf{x} + V_x^\top \delta \mathbf{x} + \mathbf{c} \quad (13)$$

where  $\mathbf{c}$  is a constant term and the derivative terms can be calculated as

$$\begin{aligned} V_x &= Q_x + \mathbf{K}Q_u + \mathbf{K}^\top Q_{uu}\mathbf{d} + Q_{ux}^\top \mathbf{d}, \\ V_{xx} &= Q_{xx} + \mathbf{K}^\top Q_{uu}\mathbf{K} + \mathbf{K}^\top Q_{ux} + Q_{ux}^\top \mathbf{K}. \end{aligned} \quad (14)$$

$V_x$  and  $V_{xx}$  at final step in the horizon ( $N$ ) can be calculated as the first and second derivatives of the final cost function ( $\ell^f$ ), respectively. In this way, derivatives of the  $Q$  function (5) for each step in the predicted trajectory can be consecutively calculated backward starting from the final step.

### B. Forward Pass

As the successive step of a backward pass to update the trajectories, forward pass implemented in [11] briefly explained here for the sake of completeness. In unconstrained situations, the forward integration starting from the initial state using the optimal linear control derived in the backward pass is sufficient to update the nominal state-control trajectories. However, the trajectories obtained by such forward integration are not guaranteed to be feasible in the existence of constraints. Therefore, deterministic state constraints obtained in the constraint tightening step (Section III-C) are also taken into account and the following QP problem is solved to find optimal deviation in control input for a single step starting from the initial state

$$\begin{aligned} \min_{\delta \mathbf{u}} \quad & Q_u^\top \delta \mathbf{u} + \frac{1}{2}(\delta \mathbf{u}^\top Q_{uu}\delta \mathbf{u}) + \delta \mathbf{x}^\top Q_{xu}\delta \mathbf{u}, \\ \text{subject to} \quad & \mathbf{g}(\mathbf{x} + \delta \mathbf{x}, \mathbf{u} + \delta \mathbf{u}) \leq 0, \\ & \mathbf{u}_{min} \leq \mathbf{u} + \delta \mathbf{u} \leq \mathbf{u}_{max} \end{aligned} \quad (15)$$

The state is then updated by forward integration using the optimal input deviation  $\delta \mathbf{u}^*$  as

$$\mathbf{x}_{k+1} = f(\mathbf{x}_k, \mathbf{u}_k + \delta \mathbf{u}^*) \quad (16)$$

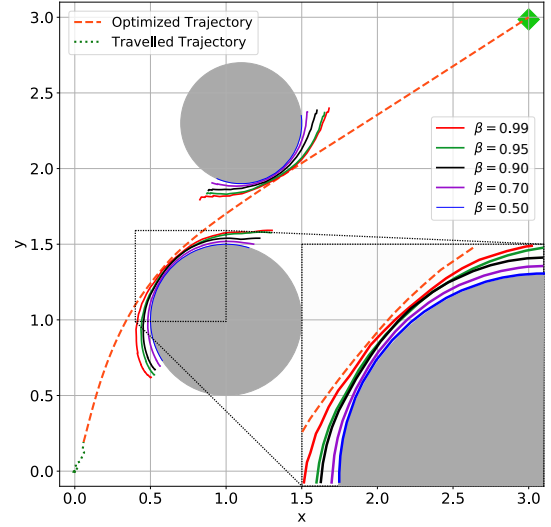


Fig. 3. Changes in the boundaries of the obstacles after tightening the constraints with different  $\beta$  values

### C. Constraint Tightening

This section explains how the chance constraints formulated in (3) are transformed into the deterministic ones which are required for backward and forward passes. In order to obtain the constraints in a deterministic form, we tighten the constraints using the propagated uncertainty through prediction, which can be decreased efficiently once a feedback policy is employed in the optimization.

Closed-loop uncertainty propagation through prediction using the control gains derived in backward pass can be approximated as:

$$\Sigma_{k+1}^x = (f_x + f_u \mathbf{K}_k)^\top \Sigma_k^x (f_x + f_u \mathbf{K}_k) + \Sigma_{k+1}^\omega \quad (17)$$

Since constrained DDP performs a local optimization at each step through prediction, general nonlinear constraint can be locally interpreted as a half-space constraint for that particular step. By utilizing the relationship between probabilistic and robust invariant sets presented in [4] for linear time-invariant systems, the effect of the propagated uncertainty could be approximately taken into account in constraint definitions for each step as follows:

$$\tilde{\mathbf{g}}(\mathbf{x}, \mathbf{u}, \Sigma^x) \triangleq \mathbf{g}(\mathbf{x}, \mathbf{u}) + \phi^{-1}(\beta) \sqrt{\mathbf{g}_x^\top \Sigma^x \mathbf{g}_x} \quad (18)$$

where  $\phi^{-1}$  is the quantile function of the standard normal distribution. Fig. 3 shows that the additional part of the right-hand side in (18) serves for altering the boundaries of the obstacles and generates safety margins based on the propagated uncertainty and the dynamics of the robot. Moreover, the  $\beta$  value adjusts the amount of uncertainty to be considered, which proportionally increases the safety limits.

Although different  $\beta$  values can be assigned for different constraints at different time steps, we did not find it beneficial for safety-required tasks and selected all the  $\beta$  values the same for simplicity.

Once all the chance-constraints are reformulated, the MPC

formulation of (3) can be written in a deterministic form as:

$$\begin{aligned}
& \min_{\mathbf{u}_0, \dots, \mathbf{u}_{N-1}} \ell^f(\mathbf{x}_N) + \sum_{k=0}^{N-1} \ell(\mathbf{x}_k, \mathbf{u}_k) \\
& \text{subject to } \mathbf{x}_{k+1} = f(\mathbf{x}_k, \mathbf{u}_k), \\
& \quad \mathbf{u}_{min} \leq \mathbf{u}_k \leq \mathbf{u}_{max}, \\
& \quad \Sigma_{k+1}^x = h(\mathbf{x}_k, \mathbf{u}_k, \mathbf{K}_k, \Sigma_k^x) \text{ Eq.(17)} \\
& \quad \tilde{\mathbf{g}}(\mathbf{x}_k, \mathbf{u}_k, \Sigma_k^x) \leq \mathbf{0}, \\
& \quad \mathbf{x}_0 = \bar{\mathbf{x}},
\end{aligned} \tag{19}$$

for all  $k = 0, \dots, N-1$ .

In order to employ a feedback policy in the optimization, Hewing *et al.* [2] restricted the policy to be a linear state feedback using pre-computed or fixed linear gains. Here, we inherently have a locally optimal affine feedback policy (11) thanks to the structure of DDP. Moreover, that policy with the controller gains derived in the backward pass (12) indeed yields a good approximation for overall nonlinear constrained DDP optimization at convergence. Consequently, the method neither needs to employ some precomputed fixed gains nor needs to solve again a finite LQR problem around the current nominal trajectory.

#### D. Algorithm in a Nutshell

Here we describe the Safe-CDDP algorithm as a whole with some practicalities to employ it in an MPC framework. Even though the initialization of such trajectory optimization algorithms is still an open problem, applying an unconstrained DDP for a relatively straightforward temporary goal state is indeed a convenient practice to initialize our method with suboptimal state-input trajectories. After initialization, our method assumes that there exists a sufficiently large safe region around the real goal state ( $\mathbf{x}_{goal}$ ) and implements a model predictive control procedure with decreasing horizon until the robot gets close to the goal state (Algorithm 1). Depending on the state dimensions, horizon length ( $N$ ) and the number of constraints, iteration number ( $n_1$ ) required to optimize the trajectory should be chosen beforehand. Once the convergence is assured,  $n_1$  can be reduced to save time and computational resources. For simplicity, we choose  $n_1 = 10$  and keep it fixed.

Solving (19) in a DDP framework revealed a chicken-egg problem, where the closed-loop uncertainty propagation requires the control gains, and the control gains are calculated in the backward pass of DDP constrained by reformulated chance-constraints using uncertainty propagation. To overcome this dilemma, we initially neglect the noise in transition dynamics at the beginning of backward and forward passes and treat the constraints as deterministic by removing the constraint satisfaction probability. Afterward, the deterministic constraints are updated via constraint tightening.

We observed that very frequent updates of closed-loop uncertainty lead to oscillations in predicted trajectories and prevent the optimizer to converge. Therefore, we suggest a slower update schedule (1 constraint updates every 5 iterations,  $n_2 = n_1/2 = 5$  as a rule of thumb) to get settled

---

#### Algorithm 1: MPC using Safe-CDDP

---

```

1 Init:  $N, \mathbf{x}_0, \mathbf{x}_{goal}, \mathbf{x}_{1,\dots,N}, \mathbf{u}_{0,\dots,N-1}$ 
2 while robot is not close to  $\mathbf{x}_{goal}$  do
3   for iter = 0, ...,  $n_1$  do
4     function BackwardPass
5        $V_x(\mathbf{x}_N) \leftarrow \ell_x^f(\mathbf{x}_N)$ 
6        $V_{xx}(\mathbf{x}_N) \leftarrow \ell_{xx}^f(\mathbf{x}_N)$ 
7       for  $k = N-1, \dots$ , do
8         Calculate derivatives of  $Q$  (Eq. 5)
9         Calculate derivatives of  $V$  (Eq. 14)
10        Save  $Q_{uu}, Q_{xu}, Q_u, K$ 
11     function ForwardPass
12        $\mathbf{x} \leftarrow \mathbf{x}_0$ 
13       for  $k = 0, \dots, N-1$  do
14          $\delta \mathbf{x} \leftarrow \mathbf{x} - \mathbf{x}_k$ 
15         Solve QP for  $\delta \mathbf{u}$  (Eq. 15)
16         if feasible solution then
17            $\mathbf{x}_{k+1} \leftarrow f(\mathbf{x}, \mathbf{u}_k + \delta \mathbf{u})$ 
18            $\mathbf{x} \leftarrow \mathbf{x}_{k+1}$ 
19         else
20           Regularization
21           break
22       if iter %  $n_2 == 0$  then
23         function ConstraintTightening
24           Calculate closed-loop uncertainty
25           propagation (Eq. 17)
26           Update constraints (Eq. 18)
27       Apply  $\mathbf{u}_0$  to robot
28        $\mathbf{x}_0 \leftarrow$  measurement
29        $\mathbf{x}_{1,\dots,N-1} \leftarrow \mathbf{x}_{2,\dots,N}$ 
30        $\mathbf{u}_{0,\dots,N-2} \leftarrow \mathbf{u}_{1,\dots,N-1}$ 
31        $N \leftarrow N-1$ 

```

---

and then update the constraints using the calculated closed-loop uncertainty as depicted in Algorithm 1.

Finally, it should be noted that the regularization scheme (line 19 in Algorithm 1) and the choice of optimization parameters such as step size and trust region in search space affect the convergence of the algorithm. In our implementation, we used a diminishing trust-region for infeasible solutions and ensured the numerical stability of matrix inversions by adding a regularization term similar to [24].

## IV. EXPERIMENTS

In this section, we present repetitive simulation results for statistical evaluation and demonstrate hardware implementation to assess the proposed method in the scope of computational feasibility and applicability to real robots.

### A. Dynamical Systems in Simulation

In this section, we statistically evaluate our Safe-CDDP algorithm on three different robot dynamics in simulation: (i) 2D point robot, (ii) 2D car-like robot, and (iii) 3D quadrotor robot. The defined task for each robot dynamics is reaching



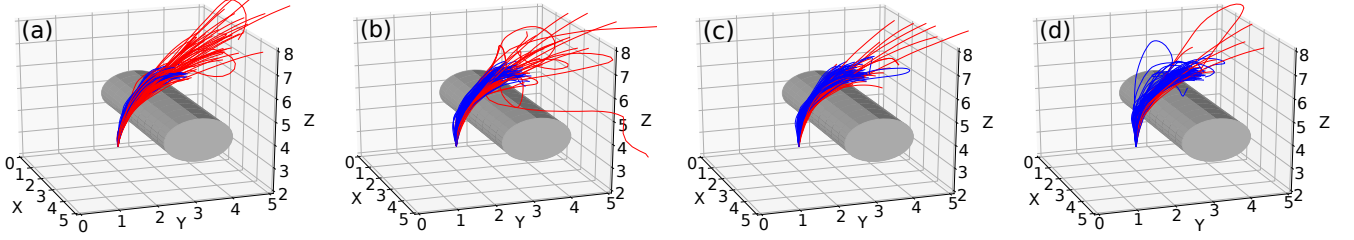


Fig. 4. Comparison of traveled trajectories of a 3D quadrotor in constrained environment. (a): Classical CDDP without safety precaution. Safe-CDDP with  $\beta$  values of (b): 0.90, (c): 0.95 and (d): 0.99. Trajectories in blue represent constraint respected ones and the ones in red for constraint violations.

a goal position while avoiding stationary obstacles. The characteristics of process noise ( $\Sigma_k^x$ ) is assumed to be known and the positions of the obstacles and the robot itself are assumed to be externally provided without noise. We also assume that there exist safe regions around the initial and goal positions. Once the robot arrived in the safe region around the goal, the task is considered successfully achieved. Another control algorithm could be subsequently triggered to maintain the robot in that region with accurate positioning, which is not a part of this study.

Stationary obstacles in the environment are formulated as circular constraints as defined in [11] and [12]. For the 3D quadrotor, it is also possible to use spherical constraints but we preferred to choose cylindrical constraints to test the performance in a more challenging scenario.

Once the task configuration is fixed for a robot, it was performed repeatedly 100 times for each of 4 different  $\beta$  values  $\{0.5, 0.90, 0.95, 0.99\}$ . Note that the case with  $\beta = 0.5$  corresponds to classical CDDP without safety precautions, since  $\phi^{-1}(0.5) = 0$ .

*a) 2D Point Robot:* Simple 2D point robot, also known as double integrator, is a linear holonomic system, where the state vector includes positions and velocities,  $\{\mathbf{x}, \mathbf{v}\}$  and the robot is assumed to be manipulated in both 2 directions by an input vector  $\mathbf{u} = [u^x, u^y]$ . The robot is initially located at (0,0) position in the environment where there exist two circular obstacles at (1,1) and (1.1, 2.3) with radius 0.5 and 0.4, respectively. Even though the final goal position of the task is set to (3,3), robot is initially targeted to (0,3) in unconstrained DDP to obtain an initial feasible safe trajectory (Algorithm 1). Control inputs are also bounded as  $|u| \leq 10$ .  $\sigma$  values of process noise for positions and velocities are set to 0.005 and 0.01, respectively. Prediction horizon  $N$  is selected as 100.

*b) 2D Car-like Robot:* Classical 2D car-like model is a simple nonlinear robot example that includes 2D position (x,y), orientation ( $\theta$ ) and the longitudinal velocity of the vehicle ( $v$ ). We consider the model presented in [11]. The task is configured very similar to 2D point robot. Control input bounds were selected as  $|u^v| \leq 10$  and  $|u^\theta| \leq \pi$ . Process noise  $\sigma$  values of positions are set to 0.001 and it is selected as 0.02 for both orientation and velocity. Since car-like robot requires non-holonomic motion to reach the goal position, longer prediction horizon ( $N = 120$ ) is selected compared to point robot.

*c) 3D Quadrotor Robot:* We lastly selected 3D quadrotor robot as a complex nonlinear dynamic system with high dimensional state space, where the state vector includes positions ( $x, y, z$ ), linear velocities ( $v^x, v^y, v^z$ ), Euler-angles ( $\phi, \theta, \psi$ ) and rotational velocities ( $p, q, r$ ). Please refer to [27] and [28] for details regarding the transformations, nonlinear dynamics and control input calculations. The robot is initially located at (2,2,3) position with (0,0,0) angles and without any linear or angular velocities. A cylindrical constrained is placed in the environments as shown in Fig. 4, where the robot is forced to move around it to reach the safe region including final goal position at (3.2, 3.2, 6.5). Initial goal for unconstrained DDP part of the algorithms was set to (1, 1, 7) position.  $N = 50$  was found to be enough in this task.  $\sigma$  values of process noise for positions/orientation and linear/angular velocities are set to be 0.001 and 0.1, respectively. Since we optimize through motor thrusts as inputs, the interval  $[0, 100]$  was selected as boundary for them.

## B. Simulation Results

In order to assess the safety of the obtained trajectories, we utilized 3 metrics regarding constraint violations (Table I). Once the robot finishes the task with either success or failure, we call it one episode and repeat the same task with a fixed configuration for 100 episodes. “Violated episode” refers to an episode in which the robot violates a constraint, *i.e.*, collides with an obstacle, at least once. Average in violated episodes is the ratio of the total number of collisions and the number of violated episodes. Similarly, the total average of violations is the ratio of the total number of collisions and the total number of episodes, *i.e.*, 100 in our case.

Table I depicts that Safe-CDDP algorithm provides safety in terms of obstacle collision due to uncertainties. By selecting  $\beta=0.99$ , Safe-CDDP performed well for point robot and car-like robot without any constraint violation, where at least one constraint violation occurred in 64 and 38 percent of the tasks for these robots when the safety precaution was removed ( $\beta=0.5$ ). Selecting  $\beta=0.95$  was even sufficient for the car-like robot to obtain safe trajectories with zero collision. This implies that increasing  $\beta$  values, *i.e.*, increasing the confidence bound on the approximated uncertainty propagation leads optimizer to be more conservative and force it to find trajectories away from the obstacles if admissible.

TABLE I  
CONSTRAINT VIOLATION RESULTS

	CDDP	Safe-CDDP			
<b>2D Point Robot</b>	$\beta=0.50$	$\beta=0.90$	$\beta=0.95$	$\beta=0.99$	
Num. of violated episodes	64	14	8	0	
Avg. in violated episodes	1.98	1.43	1.38	0	
Total avg. of violations	1.27	0.20	0.11	0	
<b>Car-like Robot</b>	$\beta=0.50$	$\beta=0.90$	$\beta=0.95$	$\beta=0.99$	
Num. of violated episodes	38	2	0	0	
Avg. in violated episodes	1.63	1.0	0	0	
Total avg. of violations	0.62	0.02	0	0	
<b>3D Quadrotor Robot</b>	$\beta=0.50$	$\beta=0.90$	$\beta=0.95$	$\beta=0.99$	
Num. of violated episodes	66	34	27	15	
Avg. in violated episodes	5.7	4.26	5.19	4.07	
Total avg. of violations	3.76	1.45	1.4	0.61	

Fig. 5 shows that the predicted trajectories around obstacles get narrower than the other regions. The main reason for this is that Safe-CDDP becomes more conservative when the robot gets closer to the constraints, and the admissible range of the states shrinks. In the regions away from the obstacles, the optimizer is free to result in any shortest path. In this figure it is also shown that the resultant safe trajectories encapsulate the transition dynamics. Safe-CDDP generates smoother and curvy trajectories for car-like robot due its non-holonomic dynamics.

It should be noted that the performance of Safe-CDDP highly depends on the admissible region of states possible for the task definition. For the 3D quadrotor robot, we deliberately select a goal position above the cylinder to assess the capabilities of the method. Fig. 4 presents all the traveled trajectories by quadrotor using Safe-CDDP with different  $\beta$  values. Once  $\beta$  is set to 0.5, *i.e.*, in the case of classical CDDP, the majority (%66) of the tasks were finished with violations. In Safe-CDDP case with  $\beta=0.99$ , collision avoidance was not satisfied completely as in the cases of point robot and car-like robot, but it is dramatically improved by diminishing from %66 to %15. This indicates that Safe-CDDP can achieve remarkable performances in decreasing the number of constraint violations for complex and under actuated systems in the presence of system uncertainties.

### C. Hardware Implementation

As an experimental setup, we employed Turtlebot3 Waffle Pi that is a differential drive type mobile robot. Typically, the transition dynamics of such robots are

$$\begin{aligned} x_{k+1} &= x_k + \delta_t u_k^v \cos(\theta_k + 0.5\delta_t u^\omega) \\ y_{k+1} &= y_k + \delta_t u_k^v \sin(\theta_k + 0.5\delta_t u^\omega) \\ \theta_{k+1} &= \theta_k + \delta_t u^\omega \end{aligned} \quad (20)$$

where  $x, y$  positions and heading angle  $\theta$  are the states of the robot controlled by linear and angular velocities ( $u^v$  and  $u^\omega$ ).  $\delta_t$  is the step time in discrete domain, which is 0.1s for our robot. In order to test Safe-CDDP on Turtlebot, we placed two circular objects with different sizes in the robot's environment as stationary obstacles. Gmapping was used to map the environment and the fusion of Adaptive Monte

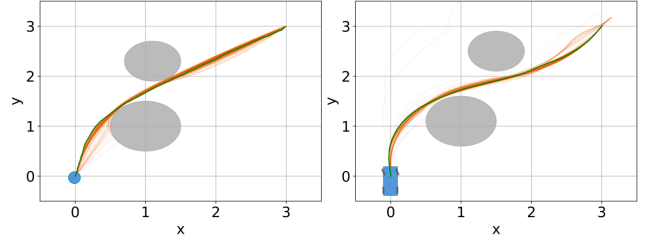


Fig. 5. Optimized safe trajectories (orange) by Safe-CDDP with  $\beta=0.99$  and traveled trajectories (green) by (Left): 2D point robot and (Right): 2D car-like robot.

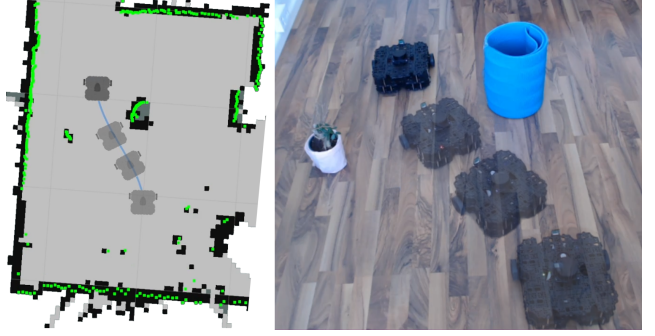


Fig. 6. Safe trajectory of Turtlebot3 optimized by Safe-CDDP.

Carlo Localization (AMCL) and odometry were employed to retrieve the states of the robot ( $x, y, \theta$ ) with an estimation uncertainty. Circular obstacles with the radius of 0.15 and 0.08 m were detected at  $(x:0.85, y:0)$  and  $(x:0.5, y:0.85)$  locations, respectively. Turtlebot was initially located in  $(x:0, y:0, \theta:0)$  and reaching to goal state  $(x:1.2, y:0.6, \theta:0)$  via Safe-CDDP was performed with the prediction horizon  $N = 90$ . Standard deviations of position noise retrieved by AMCL were approximately 0.001.

Safe-CDDP algorithm was implemented as a ROS node in C++ using OSQP [25] and Eigen [26] libraries. The execution of Safe-CDDP node was tested on both Turtlebot's CPU (Raspberry Pi-4 Model-B with 8GB RAM) and a workstation laptop (Intel i7-6820HQ CPU, 2.70GHz, 8 cores, 16GB RAM). By setting  $\beta = 0.8$ , Turtlebot was able to plan and successfully travel a safe trajectory to the goal position avoiding the obstacles with reasonable safety margins (Fig. 6) for both executions on Turtlebot's CPU and workstation laptop. The worst-case execution times of a single iteration including backward and forward pass with the trajectory length  $N = 90$  are approximately 63ms and 22ms for Raspberry Pi and workstation, respectively. Then the execution times decrease dramatically during traveling due to a decrease in active constraints and prediction horizon. This ensures the applicability of the proposed method in real robots with a control frequency faster than 10hz.

## V. CONCLUSIONS

We presented a novel safe trajectory optimization approach for nonlinear systems with nonlinear state and input constraints under additive system uncertainties. The proposed method reduces over conservatism in the approximation of uncertainty propagation through prediction. It also enables to

impose safety precautions on general nonlinear constraints. Computational feasibility and applicability of the proposed approach were shown in hardware implementation, and the effectiveness of the method was validated on three different robot dynamics in simulation.

The proposed approach approximates the future prediction uncertainty by propagating it considering the implicit gain of the DDP feedback controller. It is likely that potential approximation errors in this prediction can be compensated conservatively by increasing the safety factor. However, an exact solution would be useful to limit the need for this, but whether it is possible to find such an exact solution remains an interesting open issue.

Recently, model-based reinforcement learning (RL) has received lots of attention, and integration of optimal control with safety guarantees to systems with learned dynamics seems to offer great possibilities. The proposed approach would be applicable to data-driven models of system dynamics models when their prediction uncertainty is modeled as additive Gaussian noise, which is the case for example for Gaussian Process models. Thus, we believe that the proposed method can be integrated as a part of a RL system that would be able to provide safety guarantees also for its exploration.

#### APPENDIX

The *optimum value function*,  $V : \mathbb{R}^n \rightarrow \mathbb{R}$ , represents the minimum cost-to-go at each state and defined as:

$$V_k(\mathbf{x}_k) = \min_{\mathbf{u}_k, \dots, \mathbf{u}_{N-1}} \ell^f(\mathbf{x}_N) + \sum_{i=k}^{N-1} \ell(\mathbf{x}_i, \mathbf{u}_i), \quad (21)$$

Using Bellman's principle of optimality, the following recursive rule can be derived:

$$V_k(\mathbf{x}_k) = \min_{\mathbf{u}_k} \left[ \ell(\mathbf{x}_k, \mathbf{u}_k) + V_{k+1}(f(\mathbf{x}_k, \mathbf{u}_k)) \right], \quad (22)$$

$$V_N(\mathbf{x}_N) = \ell^f(\mathbf{x}_N).$$

The *action-value function*,  $Q : \mathbb{R}^n \times \mathbb{R}^m \rightarrow \mathbb{R}$ , evaluating the cost-to-go for a given state-action pair assuming optimal actions afterwards can be similarly defined as

$$Q_k(\mathbf{x}_k, \mathbf{u}_k) = \ell(\mathbf{x}_k, \mathbf{u}_k) + V_{k+1}(f(\mathbf{x}_k, \mathbf{u}_k)) \quad (23)$$

By taking the second-order Taylor expansion of  $Q_k$  about the nominal trajectories, the action-value function can be approximated as a quadratic function as in (4).

#### REFERENCES

- [1] T. A. N. Heirung, J. A. Paulson, J. O'Leary, and A. Mesbah, "Stochastic model predictive control—how does it work?" *Computers and Chemical Engineering*, 114, 158–170, 2018.
- [2] L. Hewing, J. Kabzan, and M. N. Zeilinger, "Cautious model predictive control using Gaussian process regression," *IEEE Transactions on Control Systems Technology*, 28(6), 2736–2743, 2019.
- [3] C. J. Ostafew, A. P. Schoellig, and T. D. Barfoot, "Robust constrained learning-based NMPC enabling reliable mobile robot path tracking," *International Journal of Robotics Research*, 35(13), 1547–1563, 2016.
- [4] L. Hewing, A. Carron, K. P. Wabersich, and M. N. Zeilinger, "On a correspondence between probabilistic and robust invariant sets for linear systems," in *European Control Conference*, 1642–1647, 2018.
- [5] B. T. Lopez, J. J. E. Slotine, and J. P. How, "Dynamic tube MPC for nonlinear systems," in *American Control Conference*, 1655–1662, 2019.
- [6] A. Majumdar, and R. Tedrake, "Funnel libraries for real-time robust feedback motion planning," *International Journal of Robotics Research*, 36(8), 947–982, 2017.
- [7] G. Lantoiné, and R. P. Russell, "A hybrid differential dynamic programming algorithm for constrained optimal control problems. part 1: Theory," *Journal of Optimization Theory and Applications*, 154(2), 382–417, 2012.
- [8] Y. Tassa, N. Mansard, and E. Todorov, "Control-limited differential dynamic programming," in *International Conference on Robotics and Automation*, 1168–1175, 2014.
- [9] J. M. S. J. Sola, and C. M. A. Santamaria-Navarro, "Squash-Box Feasibility Driven Differential Dynamic Programming," in *International Conference on Intelligent Robots and Systems*, 2020.
- [10] N. Doshi, F. R. Hogan, and A. Rodriguez, "Hybrid differential dynamic programming for planar manipulation primitives," in *International Conference on Robotics and Automation*, 6759–6765, 2020.
- [11] Z. Xie, C. K. Liu, and K. Hauser, "Differential dynamic programming with nonlinear constraints," in *International Conference on Robotics and Automation*, 695–702, 2017.
- [12] Y. Aoyama, G. Boutsellis, A. Patel, and E. A. Theodorou, "Constrained Differential Dynamic Programming Revisited," *arXiv:2005.00985*, 2020.
- [13] A. Pavlov, I. Shames, and C. Manzie, "Interior point differential dynamic programming," *IEEE Transactions on Control Systems Technology*, 2021.
- [14] T. A. Howell, B. E. Jackson, and Z. Manchester, "ALTRO: A fast solver for constrained trajectory optimization," in *International Conference on Intelligent Robots and Systems*, 2019.
- [15] E. Todorov, and W. Li, "A generalized iterative LQG method for locally-optimal feedback control of constrained nonlinear stochastic systems," in *American Control Conference*, 300–306, 2005.
- [16] E. Theodorou, Y. Tassa, and E. Todorov, "Stochastic differential dynamic programming," in *American Control Conference*, 1125–1132, 2010.
- [17] Y. Pan, and E. Theodorou, "Probabilistic differential dynamic programming," in *Advances in Neural Information Processing Systems*, 1907–1915, 2014.
- [18] O. Celik, H. Abdulsamad, and J. Peters, "Chance-Constrained Trajectory Optimization for Non-linear Systems with Unknown Stochastic Dynamics," in *International Conference on Intelligent Robots and Systems*, 2019.
- [19] N. Ozaki, S. Campagnola, R. Funase, and C. H. Yam, "Stochastic differential dynamic programming with unscented transform for low-thrust trajectory design," *Journal of Guidance, Control, and Dynamics*, 41(2), 377–387, 2018.
- [20] N. Ozaki, S. Campagnola, and R. Funase, "Tube Stochastic Optimal Control for Nonlinear Constrained Trajectory Optimization Problems," *Journal of Guidance, Control, and Dynamics*, 43(4), 645–655, 2020.
- [21] D. Q. Mayne, "Model predictive control: Recent developments and future promise," *Automatica*, 50(12), 2967–2986, 2014.
- [22] A. Bemporad, and M. Morari, "Robust model predictive control: A survey In Robustness" in *Identification and Control*, 207–226, 1999.
- [23] J. Nocedal, and S. Wright, "Numerical optimization," *Springer Science and Business Media*, 2006.
- [24] Y. Tassa, T. Erez, and E. Todorov, "Synthesis and stabilization of complex behaviors through online trajectory optimization," in *International Conference on Intelligent Robots and Systems*, 4906–4913, 2012.
- [25] B. Stellato, G. Banjac, P. Goulart, A. Bemporad, and S. Boyd, "OSQP: An operator splitting solver for quadratic programs," *Mathematical Programming Computation*, 1–36, 2020.
- [26] G. Guennebaud, and B. Jacob, "Eigen," url: <http://eigen.tuxfamily.org>, 2010.
- [27] G. Alcan, and M. Unel, "Robust hovering control of a quadrotor using acceleration feedback," in *International Conference on Unmanned Aircraft Systems*, 1455–1462, 2017.
- [28] H. Zaki, G. Alcan, and M. Unel, "Robust trajectory control of an unmanned aerial vehicle using acceleration feedback," *International Journal of Mechatronics and Manufacturing Systems*, 12(3-4), 298–317, 2019.